A Biomimetic Membrane Consisting of a Polyethyleneoxythiol Monolayer Anchored to Mercury with a Phospholipid Bilayer on Top

Lucia Becucci and Rolando Guidelli*

Department of Chemistry, Florence University, Via della Lastruccia 3, Sesto Fiorentino (Firenze), Italy

Quanying Liu, Richard J. Bushby, and Stephen D. Evans

Centre for Self-Organising Molecular Systems, University of Leeds, Leeds LS2 9JT, U.K.

Received: March 19, 2002; In Final Form: June 7, 2002

A biomimetic membrane was obtained by anchoring a hydrophilic monolayer consisting of a triethyleneoxythiol (EO3) or hexaethyleneoxythiol "spacer" to a hanging mercury drop electrode and by interposing a lipid film previously spread on the surface of an aqueous electrolyte between the spacer-coated electrode and the aqueous solution. The impedance spectrum of this biomimetic membrane and its response to the incorporation of the ion carrier valinomycin and of the physiological quinone ubiquinone-10 indicate that it has a good fluidity and consists of a stable lipid bilayer on top of the hydrophilic spacer acting as an ionic reservoir. Upon incorporation of the channel-forming polypeptide melittin, this model system exhibits a conductance entirely analogous to that reported on black lipid membranes, with the appreciable advantage of a higher stability and resistance to disruption. The surface dipole potential of the EO3 monolayer alone was obtained from the extrathermodynamic "free charge density" q_M on EO3-coated mercury, as experienced by the diffuse layer ions. The partial charge transfer from the sulfydryl group of EO3 to mercury was estimated from q_M and from the thermodynamic "total charge density" σ_M on EO3-coated mercury.

Introduction

During the past decade, several attempts have been made to realize phospholipid bilayers supported by metals and capable of incorporating integral proteins in a functionally active state. This approach has potential both for fundamental research on protein functions and for biosensor applications. To meet the above requirement, lipid bilayers should be (i) in the liquid crystalline state; (ii) in contact with an aqueous or, at least, a hydrophilic phase on both sides; and (iii) sufficiently free from defects that might provide preferential pathways for electron and ion transport across the bilayer.[1] To this end, a hydrophilic spacer terminated at one end with a sulfydryl group for anchoring to the metal surface is normally interposed between the metal and the lipid bilayer. In some cases, this "thiolspacer" is covalently bound at the opposite end to the polar head of a phospholipid molecule, giving rise to a supramolecule called "thiolipid". Self-assembly of the thiolipid on the metal surface yields half a lipid bilayer. The other half is obtained by spontaneous spreading and splitting of lipid vesicles on top of the thiolipid monolayer. Alternatively, a lipid bilayer is obtained by spontaneous spreading, without splitting, of lipid vesicles on top of a thiolspacer monolayer anchored to the metal.[2−4] Thiolspacers consisting of polyethyleneoxy[2,5−9] or oligopeptide[10−12] chains terminated with a sulfydryl group have normally been employed. Thiolipids and thiolspacers have been successfully anchored to gold and used to incorporate integral proteins by splitting or spreading of proteoliposomes.[10−16] So far, these approaches have met some difficulties in obtaining metal-supported lipid bilayers satisfactorily free of pinholes. Thus, the electrical signal following the activation of electrogenic integral proteins incorporated in the metal-supported lipid bilayer has often been found to be notably disturbed by background noise.

A thiolspacer consisting of a hexapeptide molecule with a high tendency to form a 3_{10}-helical structure was recently anchored to a hanging mercury drop electrode.[17] A phospholipid bilayer was then formed on top of the self-assembled thiolpeptide by spreading a lipid film on the surface of an aqueous solution and by interposing this film between the solution and the thiolpeptide-coated mercury drop electrode. Thanks to the defect-free surface of liquid mercury, this mercury-supported thiolpeptide/(lipid bilayer) system exhibits a differential capacity close to that of solvent-free black lipid membranes, thus denoting a very low number of pinholes and other surface defects. The present work describes some applications of a mercury-supported biomimetic membrane obtained by an analogous procedure using triethyleneoxythiol (EO3) and hexaethyleneoxythiol (EO6).

Experimental Section

Chemicals. The water used was obtained from light mineral water by distilling it once and by then distilling the water so obtained from alkaline permanganate. Merck suprapur KCl was baked at 500 °C before use to remove any organic impurities. Dioleoylphosphatidylcholine (DOPC) was obtained from Lipid Products (South Nutfield, Surrey, England). Valinomycin and melittin were purchased from Sigma and used without further purification. The other chemicals and solvents were also commercially available and used as received. EO3 and EO6 were synthesized as described elsewhere.[18,19] Dipalmitoylphosphatidylethanolamine−mercaptopropionamide (DPPE−MPA)

* Telephone: +38-055-4573097. Fax: +38-055-4573098. E-mail: guidelli@unifi.it.

10.1021/jp020742+ CCC: $22.00
Published on Web 09/12/2002

was synthesized and characterized as described elsewhere.[20] DOPC solutions were prepared by dissolving a proper amount of stock solutions of DOPC in pentane. EO3 solutions (1×10^{-3} M in ethanol) were prepared from an approximately 0.6 M suspension of EO3 in ethanol, while 1×10^{-4} M EO6 solutions in ethanol where prepared from a 7×10^{-2} M stock solution in CH_2Cl_2. These thiolspacer solutions were stored at −18 °C under argon to prevent their oxidation to disulfides, whose self-assembly on mercury is slower and less satisfactory than that of thiols. Stock solutions of 8×10^{-5} M valinomycin and of 1×10^{-3} M DPPE−MPA were prepared in chloroform and stored at 4 °C. Stock solutions of melittin in water (100 μg/mL) were freshly prepared before use. All measurements were carried out in aqueous 0.1 M KCl.

Instrumentation. A homemade hanging mercury drop electrode (HMDE) described elsewhere[21] was employed. It allows accurate changes in drop area of as little as 0.04 mm^2. Use was made of a homemade glass capillary with a finely tapered tip, about 1 mm in outer diameter. Capillary and mercury reservoir were thermostated at 25 ± 0.1 °C by the use of a water-jacketed box to avoid any changes in drop area due to a change in temperature. A glass electrolysis cell containing aqueous 0.1 M KCl and a small glass vessel containing an ethanol solution of EO3 or EO6 (or else a chloroform solution of DPPE−MPA) were placed on a movable support inside the box, as shown in Figure 1 in Tadini Buoninsegni et al.[22] The HMDE was moved vertically by means of an oleodynamic system, which ensured the complete absence of vibrations. The support was moved horizontally by a second oleodynamic system, so as to bring the desired vessel just below the HMDE.

Differential capacity and impedance spectroscopy measurements were carried out with an Autolab instrument (Echo Chemie) supplied with a FRA2 module for impedance measurements, a SCAN-GEN scan generator and GPES3 software. All potentials were measured versus a Ag|AgCl (0.1 M KCl) reference electrode but are referred to the saturated calomel electrode (SCE). Measurements of the static contact angle of water on bare mercury and on EO3- and EO6-coated mercury were carried out be the procedure described in elsewhere[23] using an automated goniometric apparatus (Ramé-Hart). Milli-Q water was used as a probe liquid, delivering the water drop, 2 μL in volume, with an automated pipetting system.

Electrode Functionalization. Self-assembly of a monolayer of EO3 or EO6 thiolspacer on the HMDE was carried out by keeping the mercury drop immersed in a small vessel containing an ethanol solution of 1×10^{-3} M EO3 or of 1×10^{-4} M EO6 for 30 min. A DOPC bilayer was then self-assembled on top of the thiolspacer monolayer by first spreading a pentane solution of DOPC on the surface of aqueous 0.1 M KCl in the electrolysis cell in an amount corresponding to five to six DOPC monolayers, and by allowing the pentane to evaporate. By use of the oleodynamic system, the thiolspacer-coated HMDE was then extracted from the vessel, and the ethanol was allowed to evaporate. The electrolysis cell was then brought below the HMDE, and the latter was lowered so as to bring it into contact with the DOPC film, taking care to keep the drop neck in contact with the lipid reservoir. This disposition allows a free exchange of material between the lipid-coated drop and the lipid reservoir on the surface of the aqueous electrolyte. Immediately after bringing the HMDE in contact with the lipid reservoir, the applied potential was repeatedly scanned, first between −0.360 and −1.060 V, and then between −0.260 and −0.660 V, while monitoring the curve of the differential capacity C versus the applied potential E, up to its stabilization. As a rule, stabilization was attained after about half an hour. Impedance $|Z(f)|$ and phase angle $\phi(f)$ between voltage and current were then recorded over the frequency range from 0.1 to 10^5 Hz, with an ac signal of 10 mV amplitude. C versus E curves and impedance spectra of an EO3- or EO6-coated HMDE were recorded by keeping the electrode completely immersed in aqueous 0.1 M KCl containing 1×10^{-3} EO3 or 1×10^{-4} M EO6, in the absence of the DOPC film on the surface of the aqueous electrolyte.

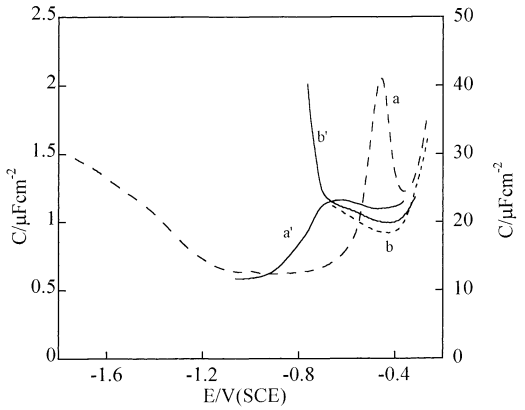

Figure 1. Plots of the differential capacity C against the applied potential E for mercury-supported monolayers of EO3 (a) and EO6 (a′), and for a DOPC film self-assembled on top of the EO3 (b) and EO6 monolayer (b′), in aqueous 0.1 M KCl. Curves a and a′ refer to the right-hand axis, curves b and b′ to the left-hand axis.

The hydrophilicity of EO3- and EO6-coated mercury electrodes was checked by measuring the contact angle of water on their surfaces. While the contact angle on bare mercury ranges from 91 to 95°, that on thiolspacer-coated mercury lies below the limits of accuracy of the automated goniometric apparatus, being <15°.

Results and Discussion

Differential Capacity and Impedance Spectroscopy Measurements. Plots of the differential capacity C against the applied potential E for mercury-supported monolayers of EO3 and EO6 in aqueous 0.1 M KCl are shown in Figure 1, curves a and a′. Both plots exhibit a narrow capacity minimum of about 12 μF cm^{-2}, which lies at about −0.8 V for EO3 and about −1.0 V for EO6. Curves b and b′ in the same figure show C versus E plots for a DOPC film self-assembled on top of the EO3 and EO6 monolayer, respectively. Here the capacity attains a flat minimum of about 1 μF cm^{-2} over the potential range from −0.35 to −0.70 V. This minimum being close to the capacity value, 0.8 μF cm^{-2}, of a solvent-free black lipid membrane[24] strongly suggests that the lipid film is actually a bilayer freely suspended on top of the thiolspacer monolayer, with the polar heads directed toward both the aqueous solution and the hydrophilic thiolspacer. This bilayer is analogous to that formed by a drop of a lipid solution in decane placed between a freshly cut hydrophilic metal,[25,26] such as Au or Ag, and an aqueous solution. In fact, the hydrophobic bare mercury surface is converted into a hydrophilic one upon coating it with a hydrophilic thiolspacer. An advantage of mercury over freshly cut Au or Ag is represented by its defect-free surface and by the mobility of the mercury surface atoms, which allows a gradual self-organization of the thiolspacer monolayer and of the overhanging lipid film during the repeated potential scans. Moreover, the lipid bilayer formed by the present procedure is free of the alkane solvent. By gradual expansion of the area of the bilayer-coated mercury drop up to twice its initial value,

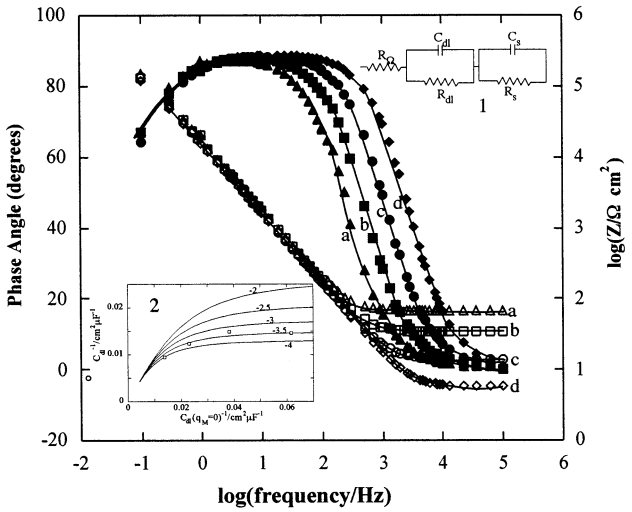

Figure 2. Plots of log|*Z*| and ϕ vs log(*f*) for an EO3-coated mercury drop immersed in 5×10^{-3} (a), 1.3×10^{-2} (b), 3.6×10^{-2} (c), and 0.1 (d) M KCl, as obtained at -0.785 V over the frequency range $0.1-10^5$ Hz. At frequencies $<10^2$ Hz, all Bode plots coincide. Open markers refer to the right-hand axis, solid ones to the left-hand axis. The solid curves are least-squares fits to the simple equivalent circuit of inset 1, which consists of the electrolyte resistance R_Ω, with, in series, a R_sC_s mesh representing the self-assembled EO3 monolayer and a further $R_{dl}C_{dl}$ mesh representing the diffuse layer. $R_s = 0.31$ MΩ cm^2; $C_s = 11$ μF cm^{-2}; $R_{dl} = 4.00$ (a),1.89 (b), 0.57 (c), and 0.10 kΩ cm^2 (d). $C_{dl} = 68$ (a), 67 (b), 82 (c), and 106 μF cm^2 (d). Inset 2 shows the reciprocal, $1/C_{dl}$, of the experimental diffuse-layer capacity vs the $1/C_{dl}$ ($q_M = 0$) value corresponding to the same KCl concentration, as calculated on the basis of the Gouy−Chapman (GC) theory. The solid curves are $1/C_{dl}$ (q_M) vs $1/C_{dl}$ ($q_M = 0$) plots calculated from the GC theory for different charge densities q_M on the metal, whose values are reported on each curve.

the differential capacity maintains a constant value of about 1 μF cm^{-2}. This proves the free exchange of lipid material between the lipid-coated mercury and the lipid reservoir on the surface of the aqueous electrolyte; the unavoidable tilting of the molecules of the thiolspacer monolayer during such an expansion has no detectable effect, because the high capacity of this monolayer makes a negligible contribution to the overall capacity of the thiolspacer/(lipid bilayer) system.

Impedance spectroscopy plots of log |*Z*| versus log(*f*) (Bode plot) and of the phase angle ϕ versus log(*f*) at -0.785 V for EO3-coated mercury in the presence of four different KCl concentrations are shown in Figure 2. The solid curves are least-squares fits to the simple equivalent circuit shown in inset 1 of the same figure: it consists of the electrolyte resistance R_Ω, with in series a R_sC_s mesh representing the self-assembled EO3 monolayer and a further $R_{dl}C_{dl}$ mesh representing the diffuse layer. The fitting was carried out by making the reasonable assumption that the EO3 monolayer, and hence its resistance R_s and capacity C_s, are not affected by a change in KCl concentration. The values of the C_{dl} and R_{dl} elements resulting from the best fit to the equivalent circuit in Figure 2 for different KCl concentrations, while keeping C_s and R_s constant, were therefore ascribed to the diffuse layer. Agreement between experimental and calculated curves is excellent. C_s equals 11 μF cm^{-2}, in fairly good agreement with the value obtained from phase-sensitive ac voltammetry at 75 Hz, while R_s amounts to 0.31 MΩ cm^2. This resistance, albeit relatively high, is much lower than that of long-chain *n*-alkanethiol monolayers on Hg[22] and Au,[27] which are in the gel state. Inset 2 of Figure 2 shows the reciprocal, $1/C_{dl}$, of the experimental diffuse-layer capacity against the corresponding value, $1/C_{dl}$ ($q_M = 0$), at zero charge density q_M on the metal for the same KCl concentration, as calculated on the basis of the Gouy−Chapman (GC) theory. The inset also shows $1/C_{dl}$ (q_M) versus $1/C_{dl}$ ($q_M = 0$) plots calculated from the GC theory for different absolute values of the charge density q_M on the metal. In fact, the calculated curves depend on the magnitude, but not on the sign, of q_M. The experimental points are in fairly good agreement with the calculated $1/C_{dl}$ (q_M) versus $1/C_{dl}$ ($q_M = 0$) plot corresponding to $|q_M| = 3.5$ μC cm^{-2}. It should be noted that q_M, called the "free charge density", is the charge density on the metal side of the interphase due to the surface excess of free electrons, which is experienced by the diffuse-layer ions. In the case of partial charge transfer between the adsorbate and the metal substrate, q_M does not coincide with the thermodynamically significant "total charge" σ_M, that is, the charge to be supplied to the electrode to keep the applied potential *E* constant when the electrode surface is increased by unity and the composition of the bulk phases is kept constant[28] (see below). EO3 chemisorption involves partial electron transfer from the sulfur atom of the sulfydryl group to the metal; this requires a flow of electrons away from the metal surface along the external circuit to keep the applied potential constant. This flow contributes to shift σ_M in the positive direction but has no such an effect on q_M.

To determine the sign of q_M, the EO3-coated mercury drop electrode was expanded rapidly inside a 1×10^{-3} M EO3 solution at E = -0.785 V, and the charge *Q* following such an expansion was recorded. The expansion occurs in a few milliseconds, while complete desorption of E03 from the electrode surface requires about 100 ms (see below). It is, therefore, reasonable to assume that this rapid expansion does not allow new EO3 molecules to be chemisorbed on the expanding drop, at least for the limited purpose of determining the sign of q_M. The sign of *Q* is negative, while the "total charge density" σ_M determined by the chronocoulometric technique at the same potential (see below) is positive and equal to $+13$ μC cm^{-2}, due to partial electron transfer from the adsorbed EO3 molecules to the metal. Hence, *Q* does not include the contribution arising from partial charge transfer from newly adsorbed EO3 molecules to an appreciable extent. Under these conditions, the volume of adsorbed material remains constant, and therefore the film thickness decreases accordingly, with a resulting increase in the differential capacity *C*. In practice, the charge *Q* consists of a contribution from the charge flowing as a consequence of the increase, ΔA, in drop area at constant *C*, and of a further contribution from the charge flowing as a consequence of the increase in *C* at constant *A*. It was shown elsewhere,[29] that $Q/\Delta A$ is approximately twice the charge density on an unexpanded mercury drop. Due to the lack of chemisorption of EO3 molecules during such an expansion, the charge density that is measured by this procedure is expected to be close to $2q_M$, rather than to $2\sigma_M$. The average value of $Q/\Delta A$ over 10 drop expansions amounts to -6 μC cm^{-2}. Even though this drop expansion measurement is quite inaccurate, since it relies on a number of approximate assumptions, its accuracy is sufficient to ascertain the negative sign of q_M. It is also gratifying that the absolute value of $Q/\Delta A$ is close to twice the value of 3.5 μC cm^{-2} obtained from the above diffuse-layer capacity measurements at -0.785 V.

Noting that the differential capacity C_s of the electrode at -0.785 V amounts to 11 μF cm^{-2} and that the EO3 spacer is neutral, the potential difference created by q_M across the thiolspacer is approximately given by $q_M/C_s \approx -0.320$ V. Neglecting the small potential difference across the diffuse layer

created by q_M in aqueous 0.1 M KCl, the whole potential difference ψ across the mercury/water interface is given by -0.320 V plus the surface dipole potential χ_s of the chemisorbed EO3 monolayer. It was shown elsewhere that the extrathermodynamic potential difference ψ at any given applied potential E measured versus a SCE can be roughly estimated by adding about $+0.250$ V to E.[30] Hence, the ψ value at -0.785 V is about -0.535 V. It follows that the surface dipole potential χ_s of EO3 is roughly equal to -200 mV. A confirmation of these estimates will be provided below, in connection with the incorporation of melittin in the lipid bilayer.

Figure 3 shows plots of $\log|Z|$ and ϕ versus $\log(f)$ for EO3-coated mercury with a DOPC bilayer on top, at -0.465 V in 0.1 M KCl. In this case, the impedance spectrum was least-squares fitted to an equivalent circuit consisting of the electrolyte resistance R_Ω, with in series the R_sC_s mesh and a further R_mC_m mesh representing the lipid film. For simplicity, the diffuse-layer $R_{dl}C_{dl}$ mesh was disregarded in view of its negligible contribution to the impedance response in the presence of the low capacity, C_m, of the lipid film and of the relatively high 0.1 M KCl concentration. In the fitting, R_s and C_s were kept fixed at the values estimated from the least-squares fit of Figure 2. Only a slight improvement in the fit was obtained by leaving these circuit elements free to change or by excluding R_m from the equivalent circuit. The fit yields a C_m value of 1.1 μF cm^{-2} and a R_m value of 0.33 MΩ cm^2, confirming the formation of a self-assembled DOPC bilayer freely suspended on top of the EO3 spacer.

For integral proteins incorporated in the metal-supported lipid bilayer to maintain a functionally active state, the hydrophilic spacer must act as a satisfactory reservoir of water and inorganic ions. To verify the fulfillment of this requirement, a simple but valuable test was adopted, which consists of incorporating the ion carrier valinomycin in the lipid layer. In the presence of an ionic reservoir interposed between the lipid bilayer and the mercury surface, the incorporation of valinomycin is expected to cause an appreciable decrease in the resistance R_m of the bilayer. In fact, the total current J comprised an ionic contribution J_{ion} and the displacement current $\partial\tilde{D}(x)/\partial t$, where $\tilde{D} = De^{i\omega t}$ is the ac electric displacement:

$$J = J_{ion} + \partial\tilde{D}(x)/\partial t = J_{ion} + i\omega\tilde{D}(x) \qquad (1)$$

In the case of a hydrophobic spacer, the ionic current J_{ion} due to inorganic ions is vanishingly small within the spacer. Consequently, the total current J is in quadrature with the ac electric displacement, as well as with the ac voltage, $\tilde{V} = \tilde{D}l/\epsilon$, where ϵ and l are the dielectric constant and the length of the film. Hence, with a hydrophobic spacer, no decrease in R_m is expected upon valinomycin incorporation, but only an increase in C_m, due to the to and fro movement of the K^+ ions caged into the valinomycin molecules within the lipid bilayer. Conversely, a hydrophilic spacer acts as an ionic reservoir, causing J_{ion} to be different from zero and J to have a nonzero in-phase component. This is the case with the EO3 thiolspacer. In fact, upon incorporating valinomycin in the DOPC bilayer on top of the spacer, an appreciable change in the impedance spectrum is observed, as appears in Figure 4. The Bode plot shows a small but appreciable inflection between two rectilinear sections of almost -1 slope at a frequency of about 10^2 Hz. Over the same frequency range, the $\phi(f)$ versus $\log(f)$ plot shows a clear minimum between two maxima. This behavior indicates that, as the frequency is progressively decreased approaching 10^2 Hz, the impedance control tends to pass from the C_m element to the R_m element, causing the slope of the Bode plot to tend to

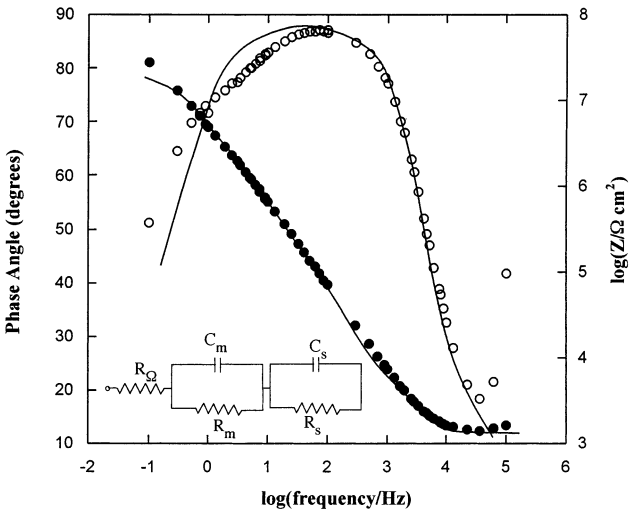

Figure 3. Plots of $\log|Z|$ (●) and ϕ (○) vs $\log(f)$ for a DOPC bilayer self-assembled on top of EO3-coated mercury, as obtained in aqueous 0.1 M KCl at -0.465 V over the frequency range $0.1-10^5$ Hz. Solid circles refer to the right-hand axis, open ones to the left-hand axis. The solid curves are least-squares fits to the equivalent circuit shown in the inset: $R_s = 0.31$ MΩ cm^2, $C_s = 11$ μF cm^{-2}, $R_m = 0.33$ MΩ cm^2, $C_m = 1.1$ μF cm^{-2}, $R_\Omega = 31$ Ω cm^2.

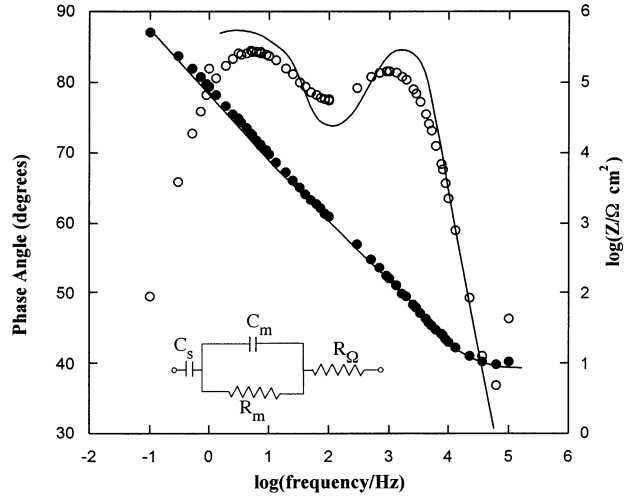

Figure 4. Plots of $\log|Z|$ (●) and ϕ (○) vs $\log(f)$ for a DOPC bilayer self-assembled on top of EO3-coated mercury, as obtained at -0.465 V in aqueous 0.1 M KCl containing 1×10^{-7} M valinomycin. Solid circles refer to the right-hand axis, open ones to the left-hand axis. The solid curves are least-squares fits to the equivalent circuit shown in the inset: $C_s = 3$ μF cm^{-2}, $R_m = 780$ Ω cm^2, $C_m = 1.9$ μF cm^{-2}, $R_\Omega = 28$ Ω cm^2.

the zero value. Much before this can occur, however, the impedance control passes to a further capacitive element of higher capacity, C_s, which can be identified with the capacity of the EO3 spacer, regarded as an ionic reservoir. Following Steinem et al.[7] and Raguse et al.,[8] the Bode plot and the $\phi(f)$ versus $\log(f)$ plot were, therefore, fitted to an equivalent circuit which differs from that of Figure 3 by the exclusion of the resistance R_s of the thiolspacer, as shown in the inset of Figure 4. The fitting shows that the incorporation of valinomycin causes a slight increase in the bilayer capacity C_m from 1.1 to 1.9 μF cm^{-2} and a drastic decrease in its resistance R_m from 0.33 MΩ cm^2 to 780 Ω cm^2. The calculated value for C_s is about 3 μF cm^{-2}. This value is somewhat lower than the value, 11 μF cm^{-2}, obtained from Figure 2. It is not clear whether this difference is real or is merely due to the use of a different equivalent circuit. The inflection in the Bode plot is small because the capacity

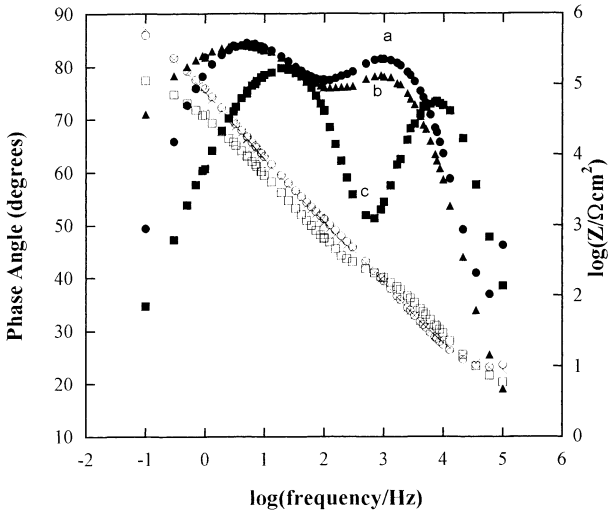

Figure 5. Plots of log|*Z*| and ϕ vs log(*f*) for a DOPC bilayer self-assembled on top of mercury-supported EO3 (a: ●, ○), EO6 (b: ▲, ×) and DPPE−MPA (c: ■, □), as obtained at −0.465 V in aqueous 0.1 M KCl containing 1×10^{-7} M valinomycin. Open markers refer to the right-hand axis, solid ones to the left-hand axis.

C_s of the spacer is only slightly higher than that, C_m, of the phospholipid bilayer. The fitting might be considerably improved by replacing the capacitive elements by constant phase elements (CPEs). However, the use of CPEs was avoided because of the dubious physical significance of a CPE in the present case. It should be noted that the fitting of impedance spectra is model-dependent and may be improved in different ways by increasing the number of circuit elements. However, the choice of the equivalent circuit must reflect a physically significant situation. Thus, for instance, an appreciable improvement in the fitting might be obtained by including the resistance R_s of the thiolspacer in the equivalent circuit, as done in the fittings of Figures 2 and 3. In this case, however, the least-squares fitting associates the higher capacity C_s, which controls the impedance at the lower frequencies, with a resistance R_s close to 1 kΩ cm^2, leaving the resistance R_m associated with the lower capacity C_m practically unaltered with respect to its value in the absence of valinomycin. This is clearly a nonphysical result, since the hydrophobic valinomycin cannot have such a large depressing effect on the resistance of the thiolspacer and no effect at all on that of the lipid bilayer. Among other things, for the resistance of a monolayer adjacent to the metal surface to be low, the ionic current J_{ion} across the interface between this monolayer and the metal must be high, in view of eq 1. Conversely, under the present conditions, J_{ion} can only be determined by charged trace impurities either electroactive (say, amalgam-forming metal ions) or capable of being adsorbed on the metal surface. These impurities may indeed be responsible for the relatively high resistance R_s estimated in the absence of valinomycin, but not for a resistance as low as 1 kΩ.

It should also be noted that the extent of the inflection in the Bode plot and of the associated pit in the $\phi(f)$ versus log(*f*) plot is not a measure of the effectiveness of the ionic reservoir represented by the hydrophilic spacer. On the contrary, Figure 5 shows that both inflection and pit decrease slightly in passing from EO3 to the longer EO6 spacer, while they increase appreciably using the DPPE−MPA spacer, whose hydrophilic portion consists of the short MPA group. This behavior is readily explained by considering that the more pronounced the inflection, the higher the capacity C_s of the spacer with respect to that, C_m, of the lipid bilayer. At a parity of polarizability, the capacity C_s of the spacer increases with a decrease in its length and, therefore, in its effectiveness as an ionic reservoir. Naturally, in the case of a mixed bilayer consisting of a long-chain *n*-alkanethiol anchored to the mercury surface with a lipid monolayer on top, neither inflection in the Bode plot nor pit in the $\phi(f)$ versus log(*f*) plot is observed because the thiolspacer, albeit long, has no hydrophilic portions.

Partial Charge Transfer from the EO3 Thiolspacer to Mercury. EO3 chemisorption on mercury is accompanied by partial charge transfer from the sulfur atom to mercury and by a partial deprotonation of the sulfydryl group. The partial charge transfer can be approximately estimated by measuring both the thermodynamically significant "total charge density" σ_M on the metal and the extrathermodynamic "free charge density" q_M experienced by the diffuse-layer ions. σ_M can be obtained by measuring the charge that accompanies a potential jump from a potential where the adsorbate is chemisorbed to one where it is completely and rapidly desorbed. As distinct from σ_M, the estimate of q_M requires extrathermodynamic assumptions. Thus, for instance, in the preceding section q_M was determined at −0.785 V by making use of the modelistic Gouy−Chapman theory. In the absence of partial charge transfer, σ_M and q_M are expected to coincide, while in its presence they will usually differ to a notable extent. The approximate procedure adopted to determine the extent of partial charge transfer of thiols at a given applied potential from the σ_M and q_M values measured at that potential is described elsewhere.[30] Briefly, let the partial charge-transfer coefficient be denoted by λ and the degree of dissociation of the sulfydryl groups by α. Taking into account that partial electron transfer from the sulfydryl groups and their deprotonation are strictly correlated events, λ and α can be regarded as approximately equal. With this assumption, it can be shown that the free charge density is given by $q_M = (\sigma_M + \lambda\sigma_i)$.[30] Here, σ_i is the charge density that would correspond to total electron transfer from the sulfydryl groups to mercury, i.e., $-eN$, where N is the number density of the chemisorbed EO3 molecules. The cross-sectional area of an EO3 molecule in its most extended configuration, as estimated from a space-filling model, amounts to ∼ 22 Å^2. Setting $N = (22\ \text{Å}^2)^{-1}$, σ_i is approximately equal to $-70\ \mu$C cm^{-2}.

The thermodynamic measurement of σ_M at a potential at which the thiol is adsorbed with partial charge transfer can be carried out if a potential at which the thiol is completely desorbed is experimentally accessible. In the present case, the plot of the differential capacity *C* versus *E* at a bare Hg electrode and that at a EO3-coated one, with both electrodes being immersed in aqueous 0.1 M tetramethylammoniun chloride (TMACl), merge at negative potentials of −1.800 V, indicating that EO3 is completely desorbed at these negative potentials. This allows the absolute charge density σ_M on EO3-coated mercury to be determined over the whole potential range of stability of the EO3 monolayer by the procedure described in elsewhere.[30] The charge involved in a potential step on bare Hg from the potential of zero charge (pzc) of aqueous 0.1 M TMACl, −0.450 V,[31] to −1. 850 V equals $-23\ \mu$C cm^{-2}: it provides the charge density, σ_M (−1.850 V), at the latter potential both on bare and on EO3-coated mercury. The charge density $Q = \sigma_M$ (−1.850 V) − σ_M (−0.785 V) following a potential step on EO3-coated mercury from −0.785 to −1.850 V amounts to $-36\ \mu$C cm^{-2}. It was obtained by extrapolating the linear and almost horizontal portion of the potentiostatic curve of $Q(t)$ versus the time *t* elapsed from the instant of the potential step to $t = 0$. Due to the relatively slow desorption of the EO3 monolayer, the linear portion of the $Q(t)$ versus *t* curve was only attained for $t > 0.120$ s. The total charge density σ_M

(−0.785 V) on EO3-coated Hg at −0.785 V is, therefore, equal to +13 μC cm^{-2}. The charge density q_M (−0.785V) experienced by the diffuse-layer ions at −0.785 V on EO3-coated mercury was already estimated from electrochemical impedance measurements (see Figure 2) and amounts to −3.5 μC cm^{-2}. The partial charge-transfer coefficient $\lambda \approx (q_M - \sigma_M)/\sigma_i$ is, therefore, approximately equal to 0.24. This denotes an incomplete electron transfer from the sulfydryl group of EO3 to mercury. This behavior differs from that exhibited by the oligopeptide thiol-spacer used elsewhere,[17] whose chemisorption on mercury is characterized by a practically complete charge transfer. Naturally, the partial charge transfer coefficient for EO3 chemisorption may be somewhat underestimated if the EO3 molecules are chemisorbed in a not fully extended configuration.

Incorporation of Ubiquinone-10. To verify the fluidity and flexibility of the mercury-supported EO3/(DOPC bilayer) system, 0.5 mol % ubiquinone-10 was incorporated in the DOPC bilayer, and the cyclic voltammogram due to its electroreduction to ubiquinol and to the reoxidation of the latter to ubiquinone was recorded. As already observed with a DOPC monolayer self-assembled directly on a HMDE[32] and with a DOPC bilayer self-assembled on a thiolhexapeptide monolayer anchored to a HMDE,[17] the cyclic voltammogram of ubiquinone exhibits a reduction peak of UQ to UQH_2 and the corresponding oxidation peak, whose peak potentials approach each other with a decrease in scan rate (data not shown). The midpoint potential, which measures the formal potential of the UQ/UQH_2 couple, shifts by about 60 mV toward more positive values per each unitary decrement of pH. Extrapolation of this potential to pH 7 yields a value of +0.110 V/NHE, in good agreement with literature values.[33] The above results indicate that the EO3/(lipid bilayer) system is fluid and flexible enough to be permeated by a hydrophobic molecule such as UQ. Practically identical results were obtained by using EO6 in place of EO3.

Incorporation of Melittin. The polypeptide melittin is the major component of the venom of the honey bee. In dilute aqueous electrolytes, melittin is monomeric, while at higher salt concentrations it forms tetrameric aggregates.[34−37] From its aqueous solutions, melittin binds spontaneously to biomembranes and black lipid membranes (BLMs). At low concentrations, it induces voltage-gated channels in BLMs, while at concentrations approximately higher than 1.2 μg/mL it causes their disruption.[38] When bound to lipid bilayers, melittin adopts a highly α-helical conformation, with most hydrophobic residues on one side and most hydrophilic residues on the opposite side of the helix long axis. At zero voltage, these amphipathic helices are commonly believed to accumulate on the surface of the membrane, parallel to the plane of the bilayer. As the voltage is made negative on the opposite side of the membrane with respect to melittin, the helices form membrane-spanning aggregates that induce pore conductance. Melittin-induced conductance G in DOPC BLMs was found to depend on voltage V and upon the concentrations of monomeric melittin and of NaCl in the aqueous solution according to the following equation:[38]

$$\log G(c, [\mathrm{NaCl}]) = \log G_0 + m \log\left(\frac{c}{c_0}\right) + n \log\left(\frac{[\mathrm{NaCl}]}{[\mathrm{NaCl}]_0}\right) - \frac{\alpha F V}{2.3RT} \quad (2)$$

with $3 < m < 4$, $n \approx 0.5$, and $\alpha = 1.1$. Here, c is the melittin concentration in the monomeric form, m and n are empirical dimensionless parameters expressing the power-law dependence of G upon c and [NaCl], and G_0 is the conductance for $c = c_0$ and [NaCl] = $[\mathrm{NaCl}]_0$. V is the electric potential on the BLM side opposite to that bathed by the melittin aqueous solution with respect to that on the same side. The number n was found to decrease from 4 to 3 going to NaCl concentrations lower than 0.4 M.

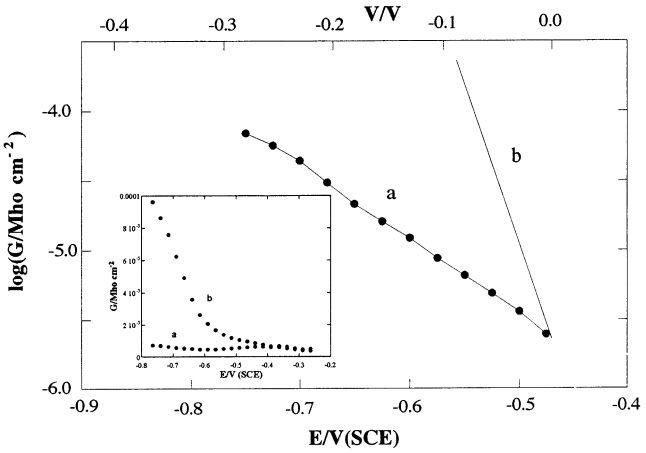

Figure 6. Curve a is a plot of log G vs E for a DOPC bilayer self-assembled on top of EO3-coated mercury, as obtained in aqueous 0.1 M KCl containing 4 μg/mL melittin. Curve b is a plot of log G vs the transmembrane potential V for a DOPC BLM, estimated as described in the text from Figure 4 in Pawlak et al.[38] The inset shows plots of G vs E in aqueous 0.1 M KCl both in the absence (a) and in the presence of 4 μg/mL melittin (b).

Melittin was incorporated in a mercury-supported EO3/(DOPC bilayer) film from a 0.1 M KCl aqueous solution containing 4 μg/mL melittin, upon stirring the solution for 5 min. The inset of Figure 6 shows the conductance G of the film as a function of the applied potential E, both in the absence and in the presence of melittin. G was directly obtained from the in-phase admittance at 10 Hz, by subtracting the admittance in the absence of melittin from that in its presence at each applied potential. The plot of log G versus E in Figure 6, curve a, is linear, indicating that G increases exponentially with a negative shift in E. This behavior is analogous to that reported in DOPC BLMs.[38] A practically identical behavior was observed over the frequency range from 0.1 to 1000 Hz, in agreement with Pawlak's finding[38] that in a melittin-doped DOPC BLM the current rise following a voltage step is very fast, in the millisecond range or below. The melittin concentration adopted herein is somewhat higher than that, ∼1.2 μg/mL, causing BLM disruption, thus confirming the ruggedness of metal-supported lipid bilayers. To compare the behavior of the log G versus E plot obtained herein with that on a DOPC BLM under the same experimental conditions, use was made of eq 2, taking into account that in a 0.1 M KCl solution melittin is entirely monomeric and m is about equal to 3. The linear plot of log G versus V for a DOPC BLM bathed on one side by a 1.8 M NaCl solution containing 1.2 μg/mL melittin (Figure 4 in Pawlak et al.[38]) is such that its extrapolation to $V = 0$ yields a log G value of −6.6, with G in mho cm^{-2}. The linear plot b of log G versus V in Figure 6 was calculated from eq 2 for $c = 4$ μg mL^{-1} and [KCl] = 0.1 M by setting log G_0 ($c = 1.2$ μg ml^{-1}, [NaCl] = 1.8 M) = -6.6, $m = 3$, $n = 0.5$, and $\alpha = 1.1$. The slope of the experimental plot a is lower than that of the calculated plot b for a DOPC BLM because the potential difference across the DOPC bilayer is equal to $(E - iR) + K$, where iR is the ohmic drop across the EO3 spacer and K is a constant that depends on the choice of the reference electrode. The two linear plots a and b were shifted along the horizontal axis in order to make them intersect at the very low log G value, −5.65, corresponding to a zero voltage V in a BLM. At this

low conductance, the ohmic drop across the EO3 spacer in the log G versus E plot a can be regarded as negligible. The E value corresponding to a zero potential difference V across the DOPC bilayer incorporating melittin amounts to about -0.460 V. In view of the extrathermodynamic estimate of the absolute potential difference ψ across a mercury/water interface,[30] $V = 0$ corresponds to a ψ value of about -200 V. Upon disregarding the small potential difference across the diffuse layer, the ψ value for $V = 0$ is expected to be approximately equal to the surface dipole potential χ_s of the EO3 thiolspacer. Hence, the ψ value for $V = 0$ being equal to -0.200 V confirms the previous estimate of χ_s. It should be noted that melittin cannot form channels in lipid monolayers directly self-assembled on mercury,[39] where it can only be adsorbed at the interface between the polar and the hydrocarbon tail regions.

In conclusion, it has been shown that a polyethyleneoxythiol anchored to a HMDE, with a self-assembled phospholipid bilayer on top, constitutes a valid experimental model of a biomembrane. Its response to the incorporation of the ion carrier valinomycin and of the physiological quinone ubiquinone-10 as well as its impedance spectrum indicate that this membrane model has a good fluidity and consists of a stable lipid bilayer on top of a hydrophilic spacer acting as an ionic reservoir. Upon incorporation of the channel-forming polypeptide melittin, this model system exhibits a conductance that is entirely analogous to that reported on black lipid membranes, with the appreciable advantage of a higher stability and resistance to disruption.

Acknowledgment. This work was financially supported by the Ministero dell'Universita' e della Ricerca Scientifica e Tecnologica. Thanks are due to Dr. Barbara Mecheri for contact angle measurements and to the Ente Cassa di Risparmio di Firenze for a fellowship to L.B.

References and Notes

(1) Guidelli, R.; Aloisi, G.; Becucci, L.; Dolfi, A.; Moncelli, M. R.; Tadini Buoninsegni, F. *J. Electroanal. Chem.* **2001**, *504*, 1.

(2) Williams, L. M.; Evans, S. D.; Flynn, T. M.; Marsh, A.; Knowles, P. F.; Bushby, R. J.; Boden, N. *Langmuir* **1997**, *13*, 751; *Supramolecular Sci.* **1997**, *4*, 513.

(3) Toby, A.; Jenkins, A.; Bushby, R. J.; Boden, N.; Evans, S. D.; Knowles, P. F.; Liu, Q.; Miles, R. E.; Ogier, S. D. *Langmuir* **1998**, *14*, 4675.

(4) Steinem, C.; Janshoff, A.; Ulrich, W. P.; Sieber, M.; Galla, H.-J. *Biochim. Biophys. Acta* **1996**, *1279*, 169.

(5) Lang, H.; Duschl, C.; Vogel, H. *Langmuir* **1994**, *10*, 197.

(6) Duschl, C.; Liley, M.; Corradin, G.; Vogel, H. *Biophys. J.* **1994**, *67*, 1229.

(7) Steinem, C.; Janshoff, A.; von dem Bruch, K.; Reihs, K.; Goossens, J.; Galla, H−J. *Bioelectrochem. Bioenerg.* **1998**, *45*, 17.

(8) Raguse, B.; Braach-Maksvytis, V.; Cornell, B. A.; King, L. G.; Osman, P. D. J.; Pace, R. J.; Wieczorek, L. *Langmuir* **1998**, *14*, 648.

(9) Cornell, B. A.; Braach-Maksvytis, V. L. B.; King, L. G.; Osman, P. D. J.; Raguse, B.; Wieczorek, L.; Pace, R. J. *Nature* **1997**, *387*, 580.

(10) Naumann, R.; Jonczyk, A.; Kopp, R.; van Esch, J.; Ringsdorf, H.; Knoll, W.; Gräber, P. *Angew. Chem., Int. Ed. Engl.* **1995**, *34*, 2056.

(11) Naumann, R.; Jonczyk, A.; Hampel, C.; Ringsdorf, H.; Knoll, W.; Bunjes, N.; Gräber, P. *Bioelectrochem. Bioenerg.* **1997**, *42*, 241.

(12) Bunjes, N.; Schmidt, E. K.; Jonczyk, A.; Rippmann, F.; Beyer, D.; Ringsdorf, H.; Gräber, P.; Knoll, W.; Naumann, R. *Langmuir* **1997**, *13*, 6188.

(13) Heyse, S.; Ernst, O. P.; Dienes, Z.; Hofmann, K. P.; Vogel, H. *Biochemistry* **1998**, *37*, 507.

(14) Schmidt, E. K.; Liebermann, T.; Kreiter, M.; Jonczyk, A.; Naumann, R.; Offenhäusser, A.; Neumann, E.; Kukol, A.; Maelicke, A.; Knoll, W. *Biosens. Bioelectron.* **1998**, *13*, 585.

(15) Heyse, S.; Stora, T.; Schmid, E.; Lakey, J. H.; Vogel, H. *Biochim. Biophys. Acta* **1998**, *85507*, 319.

(16) Naumann, R.; Schmidt, E. K.; Jonczyk, A.; Fendler, K.; Kadenbach, B.; Liebermann, T.; Offenhäusser, A.; Knoll, W. *Biosens. Bioelectron.* **1999**, *14*, 651.

(17) Peggion, C.; Formaggio, F.; Toniolo, C.; Becucci, L.; Moncelli, M. R.; Guidelli, R. *Langmuir* **2001**, *17*, 6585.

(18) Boden, N.; Bushby, R. J.; Liu, Q.; Evans, S. D.; Knowles, P. F.; Marsh, A. *Tetrahedron* **1997**, *53*, 10939.

(19) Boden, N.; Bushby, R. J.; Evans, S. D.; Toby, A.; Jenkins, A.; Knowles, P. F.; Miles, R. E. *Tetrahedron* **1998**, *54*, 11537.

(20) Krysinski, P.; Zebrowska, A.; Michota, A.; Bukowska, J.; Becucci, L.; Moncelli, M. R. *Langmuir* **2001**, *17*, 3852.

(21) Moncelli, M. R.; Becucci, L. *J. Electroanal. Chem.* **1997**, *433*, 91.

(22) Tadini Buoninsegni, F.; Herrero, R.; Moncelli, M. R. *J. Electroanal. Chem.* **1998**, *452*, 33.

(23) Slowinski, K.; Chamberlain, R. V.; Miller, C. J.; Majda, M. *J. Am. Chem. Soc.* **1997**, *119*, 11910.

(24) Montal, M.; Mueller, P. *Proc. Natl. Acad. Sci. U.S.A.* **1972**, *69*, 3561.

(25) Wardak, A.; Tien, H. T. *Bioelectrochem. Bioenerg.* **1990**, *24*, 1.

(26) Martynski, T.; Tien, H. T. *Bioelectrochem. Bioenerg.* **1991**, *25*, 317.

(27) Plant, A. L.; Gueguetchkeri, M.; Yap, W. *Biophys. J.* **1994**, *67*, 1126

(28) Frumkin, A.; Petry, O.; Damaskin, B. *J. Electroanal. Chem.* **1970**, *27*, 81.

(29) Becucci, L.; Moncelli, M. R.; Guidelli, R. *J. Electroanal. Chem.* **1996**, *413*, 187.

(30) Tadini Buoninsegni, F.; Becucci, L.; Moncelli, M. R.; Guidelli, R. *J. Electroanal. Chem.* **2001**, *500*, 395.

(31) Kimmerle, F. M.; Ménard, H. *J. Electroanal. Chem.* **1974**, *54*, 101.

(32) Moncelli, M. R.; Herrero, R.; Becucci, L.; Guidelli, R. *Biochim. Biophys. Acta* **1998**, *1364*, 373.

(33) Gordillo, G. J.; Schiffrin, D. J. *J. Chem. Soc., Faraday Trans.* **1994**, *90*, 1913.

(34) Bello, J.; Bello, H. R.; Granados, E. *Biochemistry* **1982**, *21*, 461.

(35) Terwilliger, T. C.; Eisemberg, D. *J. Biol. Chem.* **1982**, *257*, 6016.

(36) Quay, St. C.; Condie, Cl. C. *Biochemistry* **1983**, *22*, 695.

(37) Schwarz, G.; Beschiaschvili, G. *Biochemistry* **1988**, *27*, 7826.

(38) Pawlak, M.; Stankowski, S.; Schwarz, G. *Biochim. Biophys. Acta* **1991**, *1062*, 94.

(39) Miller, I. R.; Doll, L.; Lester, D. S. *Bioelectrochem. Bioenerg.* **1992**, *28*, 85.